



HAL
open science

Contribution to the study of F-G-K-M binaries. X. HD 54901, HD 120544 and HD 123280, three nearby F-type spectroscopic binaries

Jean-Michel Carquillat, Jean-Louis Prieur, Stephane Udry

► To cite this version:

Jean-Michel Carquillat, Jean-Louis Prieur, Stephane Udry. Contribution to the study of F-G-K-M binaries. X. HD 54901, HD 120544 and HD 123280, three nearby F-type spectroscopic binaries. *Astronomical Notes / Astronomische Nachrichten*, 2005, 326 (1), pp.31-37. 10.1002/asna.200410260 . hal-02111216

HAL Id: hal-02111216

<https://hal.science/hal-02111216>

Submitted on 27 Apr 2019

HAL is a multi-disciplinary open access archive for the deposit and dissemination of scientific research documents, whether they are published or not. The documents may come from teaching and research institutions in France or abroad, or from public or private research centers.

L'archive ouverte pluridisciplinaire **HAL**, est destinée au dépôt et à la diffusion de documents scientifiques de niveau recherche, publiés ou non, émanant des établissements d'enseignement et de recherche français ou étrangers, des laboratoires publics ou privés.

Contribution to the study of F-G-K-M binaries. X. HD 54901, HD 120544 and HD 123280, three nearby F-type spectroscopic binaries.

J.-M. Carquillat¹, J.-L. Prieur¹, and S. Udry²

¹ UMR 5572 d'Astrophysique, Observatoire Midi-Pyrénées – CNRS, 14, Avenue Edouard Belin, 31400 Toulouse, France.

² Observatoire de Genève, 51 chemin des Maillettes, CH-1290 Sauverny, Switzerland.

Received April 27, 2019; accepted

The orbital elements of HD 54901, HD 120544 and HD 123280, three nearby F-type spectroscopic binaries, are presented. They are based on observations made **between 1982 and 2004 with the CORAVEL instrument of Observatoire de Haute-Provence**. Physical parameters are derived for the two components of HD 54901 (SB2) and for the primaries of HD 120544 and HD 123280. The rotation-revolution synchronism of the detected components is investigated. Pseudo-synchronism is very likely **achieved by** the F7 V secondary component of HD 54901, whereas the F2/3 IV primary has not yet reached this stage.

© 0000 WILEY-VCH Verlag GmbH & Co. KGaA, Weinheim

1 Introduction

This paper is the tenth of a series (**Nadal et al., 1983, Paper I**) devoted to the study of late-type stars suspected to be spectroscopic binaries (SB) in the literature, in order to determine their orbital elements. Indeed, when we started this observing program, the statistics showed a lack of SBs with known orbits among the stars of the later spectral types (Carquillat, Ginestet & Pédoussaut 1971). Most of the observations **presented here** were obtained with the CORAVEL instrument of the Observatoire de Haute-Provence (OHP). HD 54901 and HD 123280 were previously reported as spectroscopic binaries in the General Catalogue of Stellar Radial Velocities (Wilson 1953), the main source of objects for this series. The binary nature of HD 120544 was suspected from the composite spectral classification (G5 III-IV: + A5:) given by Cowley (1973). While **this study was still in progress**, a preliminary orbit was published by Nordström et al. (1997) for HD 54901, in the context of an investigation of the radial velocities, rotations and duplicity of a large sample of F-type dwarf stars. For that star we **provide** here an improved orbit based both on our observations and on those of Nordström et al., whereas we give **the first (to our knowledge) spectroscopic orbits of HD 120544 and HD 123280**. Note that HD 54901 is a two-lined spectroscopic binary (SB2), while the two other stars are single-lined binaries (SB1).

2 Observations and derivation of the orbital elements

Most of the observations were made with the CORAVEL spectrometer mounted at the Cassegrain focus of the 1-m

Swiss telescope during the period 1982-1998, with some complementary observations of HD 120544 after this date (until 2004). This instrument allows measurements of heliocentric radial velocities (RV) by performing a cross-correlation of the stellar spectrum with a physical mask placed in the focal plane of the spectrograph (Baranne, Mayor & Poncet 1979). The RVs **thus** obtained were reduced to the RV data base system of the Geneva Observatory (Udry, Mayor & Queloz 1999). **The orbital elements were determined with our programs “BS1” and “BS2” specially designed for SB1 and SB2 systems. They are based on an iterative scheme of Gauss-Newton type that performs a least-squares minimization of the residuals, starting from an initial guess of the orbital parameters.**

For HD 54901 we used 50 observations with CORAVEL and 22 others from Nordström et al. (1997) (Table 1). Weights of 1 were assigned to the RVs of the primary component, and weights of 0.35 to those of the secondary according to their mean standard errors.

The orbital elements of HD 120544 were computed from 32 CORAVEL RVs (30 at OHP and 2 with the ESO CORAVEL at La Silla, by Andersen et al. (1985)) plus 4 RVs obtained from photographic spectra with Ila O plates) in 1985–1989 with the spectrograph mounted at the coudé focus of the OHP 1.5-m telescope (Table 2). The RVs measured from the photographic spectra, initially obtained with Fehrenbach (1972)'s tables, were corrected by an offset of $+2.9 \text{ km.s}^{-1}$ to make them consistent with CORAVEL measurements. They **were assigned a 0.3 weight** (whereas a weight of 1 was used for CORAVEL velocities), according to their mean standard error.

For HD 123280, all the 48 RVs of Table 3 **derive from** CORAVEL (OHP) observations.

The orbital elements we found are given in Table 4, and the corresponding radial velocity curves **are shown in**

The \correspondence command is obsolete!

Fig. 1. For HD 54901, the orbit we obtain confirms and improves the orbit of Nordström et al. (1997). In all cases, the standard deviation of the residuals, $\sigma_{(O-C)}$, is smaller than the mean internal error of the RVs, which indicates the absence of detectable spectroscopic third bodies in those systems.

3 Physical parameters

3.1 General procedure

In this section, we estimate some physical parameters (Table 5) from the complementary data available for those stars, mainly the parallaxes, V and $B - V$ magnitudes, and Strömgren photometry. Those three stars have parallaxes quoted in the Hipparcos catalogue (ESA 1997), which are given in Col. 4, with the corresponding errors. Those values lead to distances between 90 and 102 pc, which are small enough for the interstellar absorption effects to be neglected. The corresponding visual absolute magnitudes are given in Col. 5. Strömgren photometry measurements are also available for those stars (Hauck & Mermilliod 1998). We used the grid of Moon & Dworetzky (1985), c_0 versus β , to estimate both the effective temperature, T_{eff} (Col. 6), and the surface gravity, $\log g$ (Col. 7), of the primary components. The metallicities, $[\text{Fe}/\text{H}]$ (Col. 8) were obtained using Cayrel's relation (Crawford 1975). For the two stars for which $H\beta$ photometry was not available (HD 54901 and HD 123280), we estimated the β parameter from the $b - y$ value via the correlation relation between those two quantities as given by Crawford (1975). Finally, we report (Fig.2) the positions of the components of those systems (primaries only for HD 120544 and HD 123280, the two components for HD 54901) in the HR theoretical diagram, $\log(L/L_{\odot})$ versus $\log T_{\text{eff}}$, computed by Schaller et al. (1992) for stars of solar metallicity and completed with the isochrones computed by Meynet, Mermilliod & Maeder (1993). The absolute bolometric magnitudes required to obtain L/L_{\odot} were calculated from the values of M_v , applying the bolometric corrections tabulated by Flower (1996) for the appropriate temperatures. The positions of the stars in the HR diagram (Fig.2) lead to theoretical estimates of their masses, radius and ages, shown in Cols. 9, 10 and 11 of Table 5, respectively.

3.2 Discussion of individual cases

3.2.1 HD 54901

For this SB2, there exist some observational constraints which allow us to propose a coherent model for the system. These constraints are as follows:

- (1) The magnitude difference as deduced from the ratio of the correlation dip areas given by CORAVEL. Indeed we have the relation: $\Delta m_v = 2.5 \log[(W_1/W_2) \times (T_{\text{eff}2}/T_{\text{eff}1})]$, where W is the equivalent width, in

Table 1 Radial velocities and $(O - C)$ residuals for HD 54901. Measurements from Nordström et al. (1997) are marked with ^N

Date (JD)	Cycle	RV_1 km.s ⁻¹	$(O - C)_1$ km.s ⁻¹	RV_2 km.s ⁻¹	$(O - C)_2$ km.s ⁻¹
2400000+					
46335.68	-33.50	-27.6	-1.5	11.9	0.3
46721.69	-24.08	0.8	0.4	-22.7	0.6
46865.36	-20.58	-24.1	0.3	8.0	-1.3
47098.69	-14.89	6.4	0.7	-32.8	-2.7
47216.58	-12.01	55.1 ^N	0.7	-93.7 ^N	0.3
47461.65	-6.04	32.0	0.4	-	-
47462.93	-6.00	59.7 ^N	-0.3	-99.9 ^N	1.4
47464.97	-5.95	36.4 ^N	-1.7	-73.5 ^N	-0.8
47484.75	-5.47	-25.8 ^N	0.7	10.1 ^N	-1.9
47511.66	-4.82	-9.7 ^N	-0.9	-9.4 ^N	1.7
47542.63	-4.06	10.8 ^N	-0.8	-39.4 ^N	-1.5
47570.62	-3.38	-27.3 ^N	-0.4	11.0 ^N	-1.5
47599.52	-2.67	-19.9 ^N	0.9	7.0 ^N	2.5
47600.35	-2.65	-20.8	0.9	-	-
47607.41	-2.48	-28.0	-1.6	-	-
47640.52	-1.67	-20.5 ^N	0.3	6.5 ^N	1.9
47804.87	2.34	-19.9 ^N	1.3	5.5 ^N	0.4
47813.81	2.55	-26.5 ^N	0.2	9.8 ^N	-2.5
47821.91	2.75	-23.7 ^N	0.7	8.1 ^N	-1.1
47830.84	2.97	34.8 ^N	-0.6	-71.1 ^N	-2.0
47865.79	3.82	-20.3 ^N	-0.5	3.3 ^N	0.0
47867.64	3.87	-13.8	0.1	-4.8	-0.3
47870.68	3.94	10.4	-1.6	-38.5	-0.1
47871.58	3.96	29.0	-0.3	-	-
47872.58	3.99	54.3	0.9	-	-
47874.56	4.04	47.0	0.7	-84.1	-0.8
47896.84	4.58	-26.8 ^N	0.1	13.1 ^N	0.6
47923.72	5.23	-13.8 ^N	0.6	-	-
47955.59	6.01	61.8 ^N	0.4	-103.6 ^N	-0.4
47964.35	6.23	-13.7	-0.1	-4.5	0.4
47965.37	6.25	-17.4	-1.6	-1.0	1.0
47966.45	6.28	-18.5	-0.7	1.3	0.7
47967.39	6.30	-18.3	1.0	3.4	0.9
47969.43	6.35	-21.7	0.1	5.5	-0.4
47987.52	6.79	-22.0 ^N	0.3	8.3 ^N	1.8
48167.91	11.19	-10.4 ^N	-0.9	-9.5 ^N	0.7
48194.88	11.85	-16.3 ^N	0.5	0.6 ^N	1.3
48261.55	13.47	-27.7	-2.1	9.8	-1.1
48262.43	13.49	-26.4	-0.4	10.7	-0.7
48265.58	13.57	-27.5	-0.7	-	-
48291.67	14.21	-11.1 ^N	0.7	-9.5 ^N	-2.2
48609.80	21.97	33.2 ^N	-0.1	-65.1 ^N	1.3
48671.44	23.47	-25.8	-0.3	9.0	-1.8
48676.41	23.59	-27.0	-0.1	12.9	0.3
48937.64	29.96	30.1	1.2	-62.4	-1.9
48938.68	29.99	53.5	-0.4	-92.8	0.5
48940.55	30.03	48.6	0.6	-83.7	1.9
48967.59	30.69	-26.1	0.0	11.6	0.1
48969.57	30.74	-23.6	1.2	10.5	0.7
49325.52	39.42	-24.7	-0.3	8.8	-0.5
49427.37	41.91	-3.9	0.3	-17.3	-0.1
49428.34	41.93	6.3	0.6	-30.1	0.1
49429.36	41.95	22.2	0.1	-49.1	2.6
49430.34	41.98	44.4	-0.7	-82.9	-1.1
49431.35	42.00	61.8	-0.4	-104.6	-0.4
49432.33	42.03	52.1	-0.5	-93.4	-1.8
49432.46	42.03	49.4	-0.8	-89.1	-0.7
49640.71	47.11	7.3	0.5	-33.6	-2.0
49781.41	50.54	-26.0	0.6	-	-
49783.41	50.59	-25.2	1.7	14.0	1.5
49784.43	50.61	-26.5	0.4	13.2	0.6
49786.37	50.66	-25.7	0.9	14.4	2.3
50125.49	58.93	6.3	-0.7	-34.3	-2.4
50127.47	58.98	47.1	-0.1	-84.3	0.3
50325.66	63.81	-21.6	-1.1	2.9	-1.2
50415.62	66.01	63.3	1.1	-101.9	2.3
50418.62	66.08	18.7	1.4	-43.5	1.8
50419.60	66.11	9.0	0.9	-30.5	2.8
50420.66	66.13	0.0	-0.9	-25.3	-1.5
50477.45	67.52	-	-	12.5	0.7
50479.50	67.57	-	-	11.9	-0.5
50745.65	74.06	29.8	-0.8	-62.8	0.0

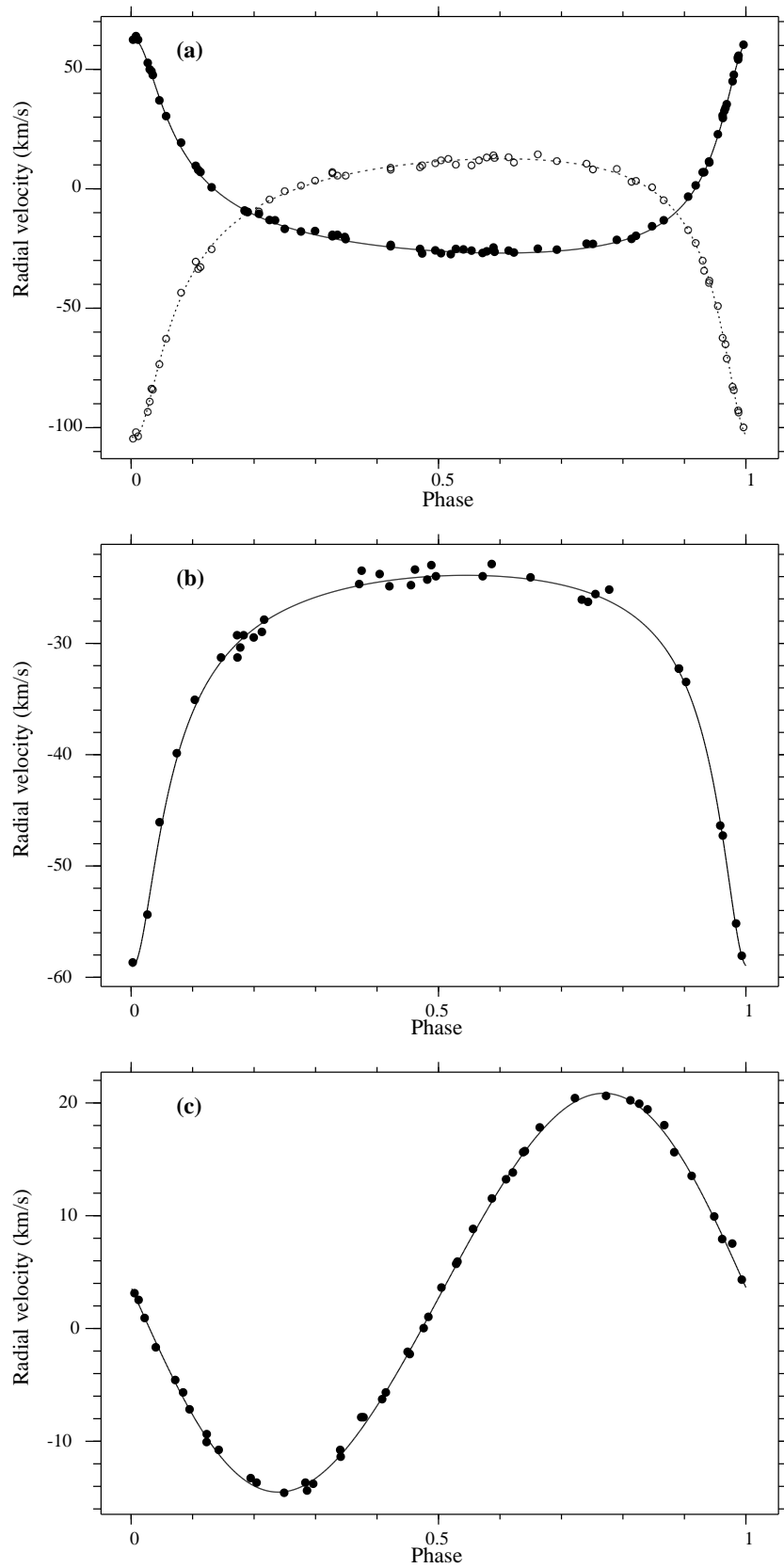


Fig. 1 RV curves computed with the orbital elements of Tables 4: (a) HD 54901, (b) HD 120544, and (c) HD 123280. The origin of the phases corresponds to the periastron passage.

Table 2 Radial velocities and ($O - C$) residuals for HD 120544. Photographic measurements are marked with P and measurements from Andersen et al. (1985) with A .

Date (JD) 2400000+	Cycle	RV km.s $^{-1}$	($O - C$) km.s $^{-1}$
44645.83	-4.26	-26.4 ^A	-1.0
44976.75	-0.54	-24.9	-0.8
44979.70	-0.51	-23.1	0.9
45127.50	1.15	-31.4 ^A	0.3
45343.74	3.57	-24.1	-0.2
46174.52	12.89	-32.4 ^P	0.1
46225.39	13.46	-23.5	0.6
46823.68	20.17	-31.4 ^P	-1.4
46901.54	21.05	-46.2 ^P	1.1
47565.64	28.50	-24.1 ^P	-0.1
47966.59	32.99	-58.2	-0.1
47969.55	33.03	-54.5	-0.6
48670.64	40.89	-32.4	0.1
48671.69	40.90	-33.6	0.3
48676.64	40.96	-46.5	-0.5
49142.42	46.18	-29.4	0.1
49145.39	46.22	-28.0	0.1
49426.62	49.37	-24.8	0.0
49429.59	49.40	-23.9	0.6
49783.56	53.37	-23.6	1.2
49787.59	53.42	-25.0	-0.7
50125.69	57.21	-29.1	-0.9
50192.53	57.96	-47.4	0.1
50194.46	57.98	-55.3	0.3
50478.68	61.17	-29.4	0.6
50610.39	62.65	-24.2	0.0
50835.73	65.18	-30.5	-0.8
50837.69	65.20	-29.6	-0.9
50974.41	66.73	-26.2	-1.0
50976.39	66.76	-25.7	0.0
50978.39	66.78	-25.3	0.9
51185.73	69.10	-35.2	0.5
52781.39	87.00	-58.8	0.2
53011.74	89.59	-23.0	0.9
53091.55	90.48	-24.4	-0.4
53144.37	91.07	-40.0	0.4

km.s $^{-1}$, of the correlation dip, and T_{eff} the effective temperature of the component, the subscripts 1, 2 referring to the primary and the secondary, respectively (Duquennoy 1994, private communication). For HD 54901, we have $W_1/W_2 = 3.48$, that leads to $\Delta m_v = 1.35$, as a first approximation assuming $T_{\text{eff}1} \sim T_{\text{eff}2}$.

- (2) The global visual absolute magnitude $M_v = 2.3$.
- (3) The global $B - V$ colour index, $B - V = 0.40$.
- (4) The mean temperature from the Strömgren photometry, $T_{\text{eff}} = 6800$ K.
- (5) The mass-ratio $K_1/K_2 = 0.76$ (Cf. Table 4).

Taking into account all those constraints, and proceeding by an iterative method, we finally obtained for the system the classification (F2/3 IV + F7 V), with $\Delta m_v = 1.25$; $T_{\text{eff}1} = 6940$ K; $T_{\text{eff}2} = 6320$ K; $M_{v1} \approx 2.6$; $M_{v2} \approx 3.9$. The theoretical masses: $M_1 \approx 1.55M_{\odot}$, $M_2 \approx 1.20M_{\odot}$ (Fig. 2) are in very good agreement with the mass-ratio deduced from the orbit. This is also close to the classification of F2 III for this system given by Nassau & MacRae (1955) from objective-prism observations.

Table 3 Radial velocities and ($O - C$) residuals for HD 123280.

Date (JD) 2400000+	Cycle	RV km.s $^{-1}$	($O - C$) km.s $^{-1}$
44979.75	-0.99	3.0	0.0
45345.72	9.07	-4.7	0.1
46226.42	33.30	-13.9	-0.5
46229.39	33.38	-8.0	0.6
46230.50	33.41	-6.4	-0.3
46486.62	40.45	-2.4	-0.4
47287.55	62.48	0.9	-0.1
47601.64	71.12	-10.2	-0.5
47604.59	71.20	-13.8	0.3
47607.48	71.28	-13.8	0.1
47609.54	71.34	-10.9	0.4
48670.72	100.53	5.6	0.0
48671.72	100.56	8.7	0.4
48673.67	100.61	13.1	-0.2
48674.68	100.64	15.5	0.0
48675.66	100.66	17.7	0.3
49140.47	113.45	-2.2	0.1
49141.42	113.48	-0.1	-0.4
49142.47	113.50	3.5	0.3
49143.42	113.53	5.8	0.0
49145.46	113.59	11.4	0.2
49147.41	113.64	15.6	-0.1
49428.57	121.37	-8.0	0.9
49781.60	131.08	-5.8	0.3
49783.71	131.14	-10.9	0.2
49785.60	131.19	-13.4	0.4
49787.58	131.25	-14.7	-0.2
49808.58	131.83	19.8	0.1
49813.48	131.96	7.8	-0.5
50164.66	141.62	13.7	-0.5
50171.61	141.81	20.1	-0.1
50172.62	141.84	19.3	0.3
50173.62	141.87	17.9	0.5
50176.57	141.95	9.8	0.0
50177.64	141.98	7.4	1.1
50193.50	142.41	-5.8	-0.2
50324.31	146.01	2.4	0.2
50325.32	146.04	-1.8	-0.6
50327.32	146.10	-7.3	-0.1
50328.34	146.12	-9.5	0.2
50479.69	150.29	-14.5	-0.7
50481.68	150.34	-11.5	-0.3
50610.48	153.88	15.5	-0.6
50611.50	153.91	13.4	-0.2
50614.47	153.99	4.2	-0.3
50615.51	154.02	0.8	-0.2
50822.74	159.72	20.3	0.2
50824.58	159.77	20.5	-0.4

3.2.2 HD 120544

Several spectral classifications in the MK system have been given for that star. In Sect. 1, we have already mentioned the composite spectral classification (G5 III-IV: + A5:) given by A. Cowley (1973). However, this first classification was never confirmed by subsequent studies. Other classifiers did not recognize a composite spectrum for HD 120544: **they only mention the spectrum of an F star alone**. Malaroda (1975) gives F7 IV, A.P. Cowley (1976) gives F7 V, and Houk & Smith-Moore (1988) give F6 IV/V. To investigate this problem, we **included** this star in our observational program of classification of stars with composite spectra in the near infrared (Ginestet et al. 1997). **Indeed** we reached the same conclusion and proposed, tentatively, the spectral type F5 V. Hence the classification proposed by A. Cowley is very probably erroneous.

With its **low mass-function** of $0.02 M_{\odot}$, the undetected secondary component of HD 120544 is likely to be faint with a low mass. Hence we have neglected its contribution

to the magnitude and photometric indices of the star, and determined the location of the primary component in the HR diagram (Fig. 2). The comparison with theoretical evolution tracks suggests this object is an already evolved star, not a dwarf, near the turn-off point. The visual absolute magnitude, close to 1.8, is consistent with the type F6 III-IV (Schmidt-Kaler 1982). Note nevertheless that the luminosity class is difficult to estimate with accuracy, from visual classifications, in the range III-V for the F stars.

3.2.3 HD 123280

The SIMBAD data base refers to only one MK spectral classification for this star, F6 V, given by Moore & Paddock (1950) from observations at Lick Observatory. Those observations also permitted to reveal the binary nature of HD 123280. **As for** HD 120544, the **low mass-function** of $0.02 M_{\odot}$ suggests a SB1 system with a faint companion, and the contribution of the secondary can be neglected. In this case, the physical parameters we find and the position in the HR diagram suggest that the primary is a bona fide dwarf star and confirm the validity of the classification F6 V.

4 Separations and minimum masses of the unseen companions

4.1 HD 54901

For this SB2, we know $a \sin i = a_1 \sin i + a_2 \sin i = 45.20$ Gm. An estimation of i can be deduced from the quantity $M_1 \sin^3 i$ and the theoretical mass $M_1 = 1.55 M_{\odot}$, i.e. $\sin i = 0.930$, or $i = 68^{\circ}$. We **thus obtain** $a = 48.60$ Gm = 0.32 a.u., which corresponds to a mean angular separation of 3.4 mas taking into account the parallax of the system. This separation makes this system resolvable with multi-pupil large interferometers.

4.2 HD 120544 and HD 123280

Writing the mass-function: $f(m) = M_1 \times \sin^3 i \times \mu^3 / (1 + \mu)^2$, where $\mu = M_2/M_1$ is the mass-ratio, we calculated for each system the minimum mass of the secondary, $M_{2\min}$, assuming for the primary the theoretical mass M_1 (Table 5, Col. 9) from the position of the star in the HR diagram. We found $M_{2\min} = 0.5 M_{\odot}$ and $0.4 M_{\odot}$ for HD 120544 and HD 123280, respectively. These masses are those of cool red dwarf stars.

For a given value of the orbital inclination i , the mean linear separation a can be computed from the following relation: $a = a_1 + a_2 = a_1 \sin i \times (1 + 1/\mu) / \sin i$, where $a_1 \sin i$ can be estimated from the orbit (Table 4, Col. 8). We have shown (Carquillat et al. 1982) that the values of a obtained using this relation are not very sensitive to the value of i , even when i varies over a large range of orbital inclinations. Hence, we calculated a for the two systems using the statistical most likely value of $i = 60^{\circ}$. For HD 120544

and HD 123280, we found $a = 76.71$ Gm = 0.51 a.u., and $a = 38.80$ Gm = 0.26 a.u., respectively. This corresponds to angular separations of 5.7 mas and 2.5 mas, respectively. **As for** HD 54901, the angular separations lie in the possibilities of optical interferometers, but in this case the low luminosity of the secondaries makes them unlikely to be detected with current available interferometers.

5 Tests of rotation-revolution synchronism

5.1 Introduction of the method

Tidal interaction between the two components of binary systems can lead either to a spiraling in of the two stars, followed by a collision, or to the evolution towards an equilibrium state characterized by circularity of the orbit, coplanarity and synchronism of the orbital and spin motions. Classically, this rotation-revolution synchronism occurs in a close system with a circular or quasi-circular orbit. Then the spin velocity $\Omega = V_e/R$ is equal to the mean angular orbital velocity $\dot{\theta} = 2\pi/P$, i.e.

$$V_e \times P = 50.6 \times R, \quad (1)$$

where V_e is the equatorial rotational velocity in km.s^{-1} , P the orbital period in days and R the radius of the star, in solar radii.

The time scales for circularization and synchronization are generally different. In detached systems where the orbital angular momentum is much larger than the rotational angular momentum at the equilibrium configuration, Hut (1981) has shown that coplanarity and synchronism of the spin and orbital motions are reached rather quickly, whereas the eccentricity of the orbit diminishes more slowly. Note that Hut's model was the "weak friction model", i.e. considering the equilibrium tide only. Zahn (1975, 1977) studied the dynamical tides, where the stars oscillate, and reached the same conclusions. Hence the orbits of binary stars are expected to remain rather eccentric for a time much longer than the time needed for synchronization.

In the case of an eccentric orbit, the tidal interaction is much more efficient near the periastron passage. Indeed, the disturbing acceleration which causes a slow change of the orbital parameters is proportional to r^{-7} , where r is the distance between the two components. Hut (1981) proposed that the synchronism is first reached in this part of the orbit only: this is the *pseudo-synchronism*. He defines the spin velocity of pseudo-synchronism Ω_{ps} as the equilibrium (minimum) value for the spin velocity obtained through energy dissipation by tidal effects, considering the present value of the eccentricity e as constant. In reality, the eccentricity decreases slowly with time, and hence Ω_{ps} is larger than Ω_{∞} , the value of the spin velocity when the full equilibrium is reached (with $e = 0$). When a component rotates with $\Omega = \Omega_{\text{ps}}$, it is qualified as "*pseudo-synchronized*". The corresponding spin period $P_{\text{ps}} = 2\pi/\Omega_{\text{ps}}$, is called

pseudo-synchronisation period. For such a system, the instantaneous angular orbital velocity at the periastron is close to (but slightly different from) Ω_{ps} .

Hut (1981) has found that:

$$P_{\text{ps}} = P \times \frac{(1 + 3e^2 + \frac{3}{8}e^4)(1 - e^2)^{3/2}}{(1 + \frac{15}{2}e^2 + \frac{45}{8}e^4 + \frac{5}{16}e^6)} \quad (2)$$

An observational test for pseudo-synchronism can be expressed by the condition that the observed angular rotation of the star is equal to Ω_{ps} :

$$\frac{V_e}{R} = \frac{2\pi}{P_{\text{ps}}} \quad (3)$$

The values of the projected equatorial velocities $V_e \sin i$ (generally called $v \sin i$), can be deduced from the profiles of the CORAVEL correlation dips, with the method described in Benz & Mayor (1981, 1984). They are given in Table 5 (Col. 3). The values of V_e remain unfortunately not accessible since the inclination i is unknown. By multiplying the two members of (3) by $\sin i$ we obtain: $v \sin i = 50.6 R \sin i / P_{\text{ps}}$ (with the same units as relation (1)). Hence

$$v \sin i \leq 50.6 R / P_{\text{ps}} \quad (4)$$

appears as a condition of pseudo-synchronism (and even of synchronism since $P_{\text{ps}} = P$ when $e = 0$), when i is unknown.

5.2 The SB1s: HD 120544 and HD 123280

For HD 120544, which has a notable eccentricity, the relation (2) gives $P_{\text{ps}} = 19.07$ d, and (4) gives $v \sin i \leq 8.5 \pm 1.0$ km.s⁻¹, which is incompatible with the value of 23.5 ± 2.4 km.s⁻¹, quoted in Table 5.

For HD 123280, which has a quasi-circular orbit, the relation (4) with $P_{\text{ps}} \approx P$ gives $v \sin i \leq 1.9 \pm 0.2$ km.s⁻¹, also incompatible with the observed value (8.6 ± 0.5 km.s⁻¹). We conclude that the primaries of those two systems rotate too fast for synchronism or pseudo-synchronism.

5.3 The SB2 HD 54901

Like HD 120544, HD 54901 has a notable eccentricity. The period of pseudo-synchronism is $P_{\text{ps}} = 8.89$ d. Applying the relation (4) to the primary, we find: $v_1 \sin i \leq 10.3 \pm 1.4$ km.s⁻¹ as a condition of pseudo-synchronism, which is not compatible with the observed value (16.3 ± 1.0 km.s⁻¹). Applying the same relation to the secondary, we find $v_2 \sin i \leq 7.1 \pm 0.9$ km.s⁻¹. For this component, the condition (4) appears to be verified by the observed value (8.5 ± 1.0 km.s⁻¹). More precisely, if we adopt for $\sin i$ the assumed value of 0.93 (see Sect. 4.1), the pseudo-synchronism hypothesis requires $v \sin i = 6.6 \pm 1.0$ km.s⁻¹, value which remains compatible with the observed value within the errors. We conclude that the secondary of HD 54901 has probably reached the state of pseudo-synchronism.

This result could be explained by the fact that the secondary, cooler than the primary, should have a thicker convective zone and consequently should be the first component to be synchronized. Indeed, theoretical works (e.g., Zahn, 1975, 1977) have shown that tidal interaction is much more effective in stars possessing a convective envelope, and the main dissipation process is then convective turbulence.

Acknowledgements. This work is based on observations made at the Haute-Provence Observatory (France).

We are indebted to M. Mayor, Director of Geneva Observatory, for giving us observing time with CORAVEL. We thank B. Pernier, J.-L. Halbwegs, M. Imbert, and R. Griffin for making some observations of HD 120544 and HD 123280 at our request. For bibliographic references, we used the SIMBAD data base, operated by the “Centre de Données Astronomiques de Strasbourg” (France).

References

- Andersen, J., Nordström, B., Ardeberg, A., Benz, W., Imbert, M., Lindgren, H., Martin, N., Maurice, E., Mayor, M., Prévot, L.: 1985, *A&AS* 59, 15
- Baranne, A., Mayor, M., & Poncet, J.L.: 1979, *Vistas Astron.*, 23, 279
- Benz, W., Mayor, M.: 1981, *A&A*, 93, 235
- Benz, W., Mayor, M.: 1984, *A&A*, 138, 183
- Carquillat, J.-M., Ginestet, N., Pédoussaut, A.: 1971, *Sciences*, Tome II-N°4, 251
- Carquillat, J.-M., Nadal, R., Ginestet, N., Pédoussaut, A.: 1982, *A&A*, 115, 23
- Cowley, A.: 1973, *PASP* 85, 314
- Cowley, A.P.: 1976, *PASP* 88, 95
- Crawford, D.L.: 1975, *AJ*, 80, 955
- ESA: 1997, *The Hipparcos and Tycho Catalogues*, ESA SP-1200, ESA Publications Division, Noordwijk
- Fehrenbach, Ch.: 1972, *A&A* 19, 427
- Flower, P.J.: 1996, *ApJ*, 469, 355
- Ginestet, N., Carquillat, J.-M., Jaschek, C., Jaschek, M.: 1997, *A&AS* 123, 135
- Hauck, B., Mermilliod, J.-C.: 1998, *A&AS*, 129, 431
- Houk, N., Smith-Moore, M.: 1988, *Catalogue of two-dimensional spectral types for the HD stars*, Ann Arbor, Dep. Astron, Univ. Michigan, Vol. 4
- Hut, P.: 1981, *A&A*, 99, 126
- Malaroda, S., 1975: *AJ* 80, 673
- Meynet, G., Mermilliod, J.-C., Maeder, A.: 1993, *A&AS*, 98, 477
- Moon, T.T., Dworetzky, M.M.: 1985, *MNRAS*, 217, 305
- Moore, J.H., Paddock, G.F.: 1950, *ApJ* 112, 48
- Nadal, R., Carquillat, J.-M., Pédoussaut, A., Ginestet, N.: 1983, *A&AS*, 52, 293 (Paper I).
- Nassau, J.J., MacRae, D.A.: 1955, *ApJ* 121, 32
- Nordström, B., Stefanik, R.P., Latham, D.W., Andersen, J.: 1997, *A&AS*, 126, 21
- Schaller, G., Schaerer, D., Meynet, G., Maeder, A.: 1992, *A&AS*, 96, 269
- Schmidt-Kaler, Th.: 1982, in *Landolt-Börnstein, Numerical Data and Functional Relationships in Science and Technology*, K. Schaifers & H.H. Voigt eds., New Series, Gr. VI, Vol. 2-b (Springer-Verlag, Berlin), pp 1–35
- Udry, S., Mayor, M., Queloz, D.: 1999, in *Precise Stellar Radial Velocities*, ASP Conferences Ser., 185, 367

Wilson, R.E.: 1953, General Catalogue of Stellar Radial Velocities, Carnegie Institution Washington Publ. 601
Zahn, J.-P.: 1975, A&A 41, 329
Zahn, J.-P.: 1977, A&A 57, 383

Table 4 Orbital elements of HD 54901, HD 120544 and HD 123280. In Col. 3, T is the epoch of periastron passage.

Name	P (days)	T 2400000+ (JD)	ω (deg.)	e	K_1 K_2 (km.s ⁻¹)	V_0 (km.s ⁻¹)	$a_1 \sin i$ $a_2 \sin i$ (Gm)	$M_1 \sin^3 i$ $M_2 \sin^3 i$ (M _⊙)	$f(m)$ (M _⊙)	$\sigma(O - C)_1$ $\sigma(O - C)_2$ (km.s ⁻¹)
HD54901 (Nordström et al. 1997)	41.00333 ±0.00125	47709.088 ±0.024	349.3 ±0.5	0.638 ±0.004	44.46 ±0.26 58.45 ±0.72	-9.86 ±0.15	- - -	- -	- -	0.72 2.36
HD54901 (this work)	41.00285 ±0.00030	47709.105 ±0.016	349.0 ±0.3	0.629 ±0.002	44.62 ±0.16 58.47 ±0.27	-9.82 ±0.10	19.56 ±0.11 25.64 ±0.16	1.245 ±0.022 0.950 ±0.018	-	0.83 1.38
HD120544	89.1477 ±0.0043	45025.31 ±0.23	175.3 ±1.0	0.634 ±0.007	17.57 ±0.22	-30.35 ±0.12	16.65 ±0.33	-	0.0232 ±0.0014	0.61
HD123280	36.35588 ±0.00060	45015.91 ±0.63	88.5 ±6.1	0.046 ±0.005	17.68 ±0.09	3.15 ±0.06	8.831 ±0.048	-	0.0208 ±0.0003	0.38

Table 5 Physical parameters of the stars belonging to the binary systems derived from observational and theoretical data (* in Col. 9: minimum value for M_2).

Star	V $B - V$	$v_1 \sin i$ $v_2 \sin i$ (km.s ⁻¹)	π (mas)	M_v	$T_{\text{eff}1}$ $T_{\text{eff}2}$ (K)	$\log g$ (cgs)	[Fe/H] (dex)	M_1 M_2 (M _⊙)	R_1 R_2 (R _⊙)	$\log(\text{age})$ (years)
HD54901	7.22 0.40	16.3 ± 1.0 8.5 ± 1.0	10.48 ±1.10	2.32 ±0.23	6940 ± 75 6320 ± 75	4.1 ±0.04	+0.04	1.55 ± 0.08 1.20 ± 0.05	1.81 ± 0.25 1.25 ± 0.17	9.15 +0.05/ - 0.05
HD120544	6.54 0.51	23.5 ± 2.4 ±0.84	11.11 ±0.17	1.77 ±0.17	6400 ± 90	4.0 ±0.09	+0.09	1.70 ± 0.08 0.48 ± 0.03*	3.22 ± 0.37	9.25 +0.1/ - 0.1
HD123280	8.64 0.47	8.6 ± 0.5 ±0.92	9.80 ±0.20	3.60 ±0.20	6450 ± 90	4.2 ±0.01	-0.01	1.30 ± 0.05 0.39 ± 0.01*	1.35 ± 0.17	9.30 +0.1/ - 0.5

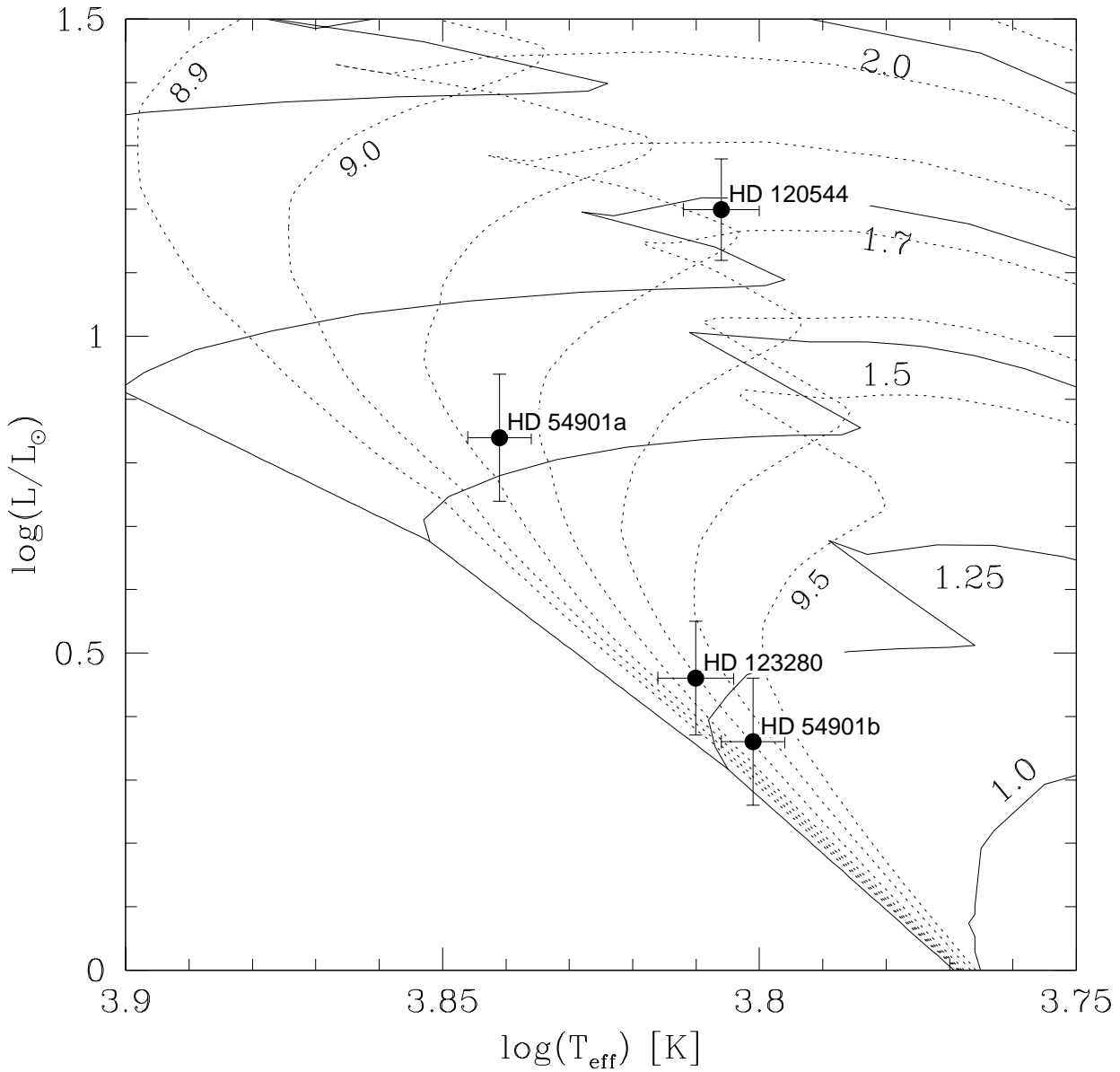


Fig. 2 Location of the components of the binary systems in the theoretical evolutionary HR diagram computed by Schaller et al. (1992) for $Z = 0.02$, with the isochrones (dotted lines) given by Meynet et al. (1993), for log age[years] varying from 8.9 to 9.5 by steps of 0.1. The solid lines correspond to the evolution tracks for mass values of 1.0, 1.25, 1.5, 1.7 and 2.0 M_{\odot} .